Article

Determination of Material Properties of Basketball. Finite Element Modeling of the Basketball Bounce Height

Andrzej Makowski [1],

[1] Faculty of Forestry and Wood Technology, Poznan University of Life Sciences, Poland
* Correspondence: andrzej.makowski@au.poznan.pl

Abstract: This paper presents a method to determine material constants of a standard basketball shell together with the development of a virtual numerical model of a basketball. Material constants were used as the basis for the hyperelastic material model in the *strain energy function* (*SEF*). Material properties were determined experimentally by strength testing in uniaxial tensile tests. Additionally, the digital image correlation technique (DIC) was applied to measure strain in axial planar specimens, thus providing input stress-strain data for the Autodesk® software. Analysis of testing results facilitated the construction of a hyperelastic material model. The optimal Ogden material model was selected. Two computer programmes by Autodesk® were used to construct the geometry of the virtual basketball model and to conduct simulation experiments. Geometry was designed using Autodesk Inventor Professional 2017®, while Autodesk Simulation Mechanical 2017® was applied in simulation experiments. Simulation calculations of the model basketball bounce values were verified according to the FIBA recommendations. These recommendations refer to the conditions and parameters which should be met by an actual basketball. A comparison of experimental testing and digital calculation results provided insight into the application of numerical calculations, designing of structural and material solutions for sports floors.

Keywords: hyperelastic materials; FEM; basketball; sports floors; Ogden model; FIBA

1. Introduction

In the production of sports balls, particularly basketballs, the shelling is typically manufactured from rubber and rubber-based materials reinforced with synthetic fibres. Such materials exhibit properties of a hyperelastic material. Constitutive compounds for such materials, which from the very beginning under loading show elastic properties, have been searched for since the 1940s [**1,2**]. The need for the mathematical description of behaviour for a hyperelastic material under strain is reflected in many contemporary constitutive material models. One of such solutions is provided by phenomenological models. They treat this problem from the point of view of continuum mechanics, as the stress-strain behaviour with no reference to the microscopic structure. Other solutions include physically motivated models, considering the reaction of the material from the point of view of microstructure. Characteristics of material model properties may be described using specific mathematical equations. The most commonly used solutions include e.g. the Mooney-Rivlin, neo-Hookean, Yeoh, Gent, Ogden, Arruda–Boyce, Zahorski or Blatz-Ko models [**3-9**]. All these theories are based on the empirical form of the *strain energy function* (*SEF*) of the material. Hyperelastic materials are characterised by the capacity to undergo considerable elastic strains under load while

Preprints (www.preprints.org) | NOT PEER-REVIEWED | Posted: 13 January 2021 doi:10.20944/preprints202101.0241.v1

at the same time retaining their original properties. As a rule they maintain a non-linear relationship between load and deformation, which is not linearly proportional. For this reason rubber-based materials are modelled as non-compressible materials, in the function of strain energy dependent on material constants and invariants of the deformation tensor. Their behaviour under load in the stress-strain function is highly non-linear and a simple modulus of elasticity is no longer sufficient to describe material characteristics. For this reason, it is of great importance to characterize elastic behaviour of highly extensible, nonlinear materials.

Assuming material isotropy and non-compressibility ($\sigma_2 = \sigma_3 = 0$) [**10-11**], the strain energy function (W) considering the invariants of the Cauchy-Green deformation tensor (I_1, I_2, I_3) may be presented as:

$$W_{isotropic} = f(I_1, I_2, I_3) \tag{1,0}$$

The phenomenological model of strain energy for a hyperelastic non-compressible material as a rule takes the form of an nth-degree polynomial. According to the Mooney-Rivlin equation originating from the continuum mechanics it may be presented as:

$$W(I_1, I_2, I_3) = \sum_{i,j,k=0}^{N} C_{ijk} (I_1 - 3)^i (I_2 - 3)^j (I_3 - 3)^k \tag{2.0}$$

here: C_{ijk} coefficients - are determined experimentally

In the case of a uniaxial tension the invariants take the form:

$$I_1 = \lambda^2 + \frac{2}{\lambda}; \qquad I_2 = 2\lambda + \frac{1}{\lambda^2}; \qquad I_3 = 1\text{- since there is no change in volume}$$

$$\lambda = 1 + \varepsilon; \qquad \lambda_1 = \lambda \; ; \; \lambda_2 = \lambda_3 = \frac{1}{\sqrt{\lambda}} \tag{3.0}$$

In the general situation the invariants defined by strains $\lambda_1, \lambda_2, \lambda_3$ along the three directions of the Cartesian coordinate system are denoted as:

$$I_1 = \lambda_1^2 + \lambda_2^2 + \lambda_3^2 \; ; \qquad I_2 = \lambda_1^2\lambda_2^2 + \lambda_2^2\lambda_3^2 + \lambda_3^2\lambda_1^2 \; ; \qquad I_3 = \lambda_1^2\lambda_2^2\lambda_3^2 \tag{4.0}$$

Generally, hyperelastic materials are considered incompressible, i.e. $I_3 = 1$; hence only two independent strain measures, namely I_1 and I_2, remain. This implies that W is a function of I_1 and I_2 only:

$$W = W(I_1 - 3, I_2 - 3) \tag{5.0}$$

The selection of an appropriate model depends in the range, within which it is planned to simulate strain. If a limited range of strain is considered, e.g. max. 10%, then the best reflection of the material properties is provided by the neo-Hookean model as a particular case of the model proposed by Rivlin:

$$W = C_{10} (I_1 - 3)^1 \tag{6.0}$$

At greater ranges of strain at 10-300%, a better approximation is given by the model developed by Mooney and Rivlin:

$$W = C_{10} (I_1 - 3)^1 + C_{01}(I_2 - 3)^1 \tag{7.0}$$

The Mooney-Rivlin form can be viewed as an extension of the neo-Hookean form in that it adds a term that depends on the second invariant of the left Cauchy-Green tensor. In some cases, this form will give a more accurate fit to the experimental data than the neo-Hookean form. In general, however, both models give similar accuracy since they use only linear functions of the invariants.

At very high strains reaching 700% a good fit may be obtained using the model proposed by Yeoh:

$$W = C_{10} (I_1 - 3)^1 + C_{20}(I_2 - 3)^2 + C_{30}(I_3 - 3)^3 \tag{8.0}$$

Preprints (www.preprints.org) | NOT PEER-REVIEWED | Posted: 13 January 2021 doi:10.20944/preprints202101.0241.v1

The selection of a material model does not provide a close representation of hyperelastic strains, as material constants of the polynomials still need to be accurately defined. They are dependent e.g. on physical measures such as Young's modulus or scleroscope (Shore's) hardness number as well as the chemical composition of the material. A reliable method to determine the indexes is to conduct experimental tests. These may include uniaxial tensile tests of the material samples, while in the case of compressive materials hydrostatic compression tests are also performed.

The aim of this study, among other things, is to investigate material properties of the ball shelling including an appropriate hyperelastic model. Adoption of such a material model will facilitate designing and performance of simulation tests for a numerical model of a basketball using the FEM approach. A novelty in this study is connected with the comparative tests for bounce from a rigid floor conducted for an actual ball and the model. The results will contribute insight into the evaluation of behaviour of various flooring structures and used materials under loading.

2. Materials and Methods

2.1. Materials *Hyperelastic models in Autodesk®*

Within the Autodesk Simulation Mechanical® programme six types of hyperelastic material models are available, such as e.g. the Mooney-Rivlin, Ogden, neo-Hookean and Yeoh models, as presented in **Figure 1**. Each model defines the strain energy function in a different manner.

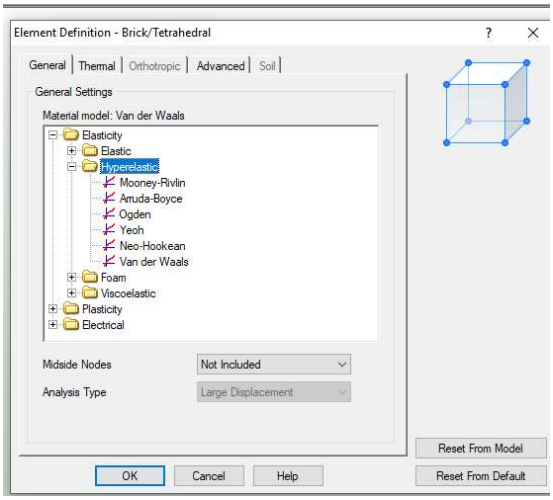

Figure 1. The Selection Window of material models in Autodesk®

A brief overview of hyperelastic models available in Autodesk® and used in the study is given below. These procedures calculate material constants based on experimentally measured stress-strain data.

2.1.1. Mooney-Rivlin model

The Mooney-Rivlin material model is a hyperelastic material model and is available for brick, tetrahedral, membrane and shell elements. It is a two-parameter phenomenological model that works well for moderately large strains in uniaxial elongation and shear deformation. For a compressible rubber, the model takes and following form and the potential function of the material for different orders is as follows:

2-constant standard:

Preprints (www.preprints.org) | NOT PEER-REVIEWED | Posted: 13 January 2021 doi:10.20944/preprints202101.0241.v1

$$W = C_{10}(\overline{I_1} - 3) + C_{01}(\overline{I_2} - 3) + \sum_{i=1}^{N} \frac{K_i}{2}(J_3 - 1)^{2i} \tag{9}$$

5-constant high-order:

$$W = C_{10}(\overline{I_1} - 3) + C_{01}(\overline{I_2} - 3) + C_{20}(\overline{I_1} - 3)^2 + C_{11}(\overline{I_1} - 3)(\overline{I_2} - 3) + C_{02}(\overline{I_2} - 3)^2 + \sum_{i=1}^{N} \frac{K_i}{2}(J_3 - 1)^{2i} \tag{10}$$

9-constant high order:

$$W = C_{10}(\overline{I_1} - 3) + C_{01}(\overline{I_2} - 3) + C_{20}(\overline{I_1} - 3)^2 + C_{11}(\overline{I_1} - 3)(\overline{I_2} - 3) + C_{02}(\overline{I_2} - 3)^2 + C_{30}(\overline{I_1} - 3)^3 + C_{21}(\overline{I_1} - 3)^2(\overline{I_2} - 3) + C_{12}(\overline{I_1} - 3)(\overline{I_2} - 3)^2 + C_{03}(\overline{I_2} - 3)^3 + \sum_{i=1}^{N} \frac{K_i}{2}(J_3 - 1)^{2i} \tag{11}$$

Regardless of the order, the initial shear modulus, μ_0, and the bulk modulus, k_0, depend only on the polynomial coefficient of order N=1:

$$\mu_0 = 2(C_{10} + C_{01}) \text{ , } k_0 = K_1 \tag{12}$$

The Mooney-Rivlin form can be viewed as an extension of the Neo-Hookean form in that it adds a term that depends on the second invariant of the left Cauchy-Green tensor. In some cases, this form will give a more accurate fit to the experimental data than the neo-Hookean form. In general, however, both models give similar accuracy since they use only linear functions of the invariants. These functions do not allow representation of the "upturn" at higher strain levels in the stress-strain curve.

2.1.2. *Neo-Hookean model*

The neo-Hookean material model is a hyperelastic material model available for 2D, brick and tetrahedral elements. This routine calculates the material constants using measured stress-strain data. This model is a special case of the Mooney-Rivlin form with C_{01}= 0 and can be used when material data is insufficient. It is simple to use and can make good approximation at relatively small strains. However, it too cannot capture the upturn of the stress strain curve. The potential function of the neo-Hookean material model is as follows:

$$W = C_{10}(\overline{I_1} - 3) + \frac{K}{2}(J_3 - 1)^2 \tag{13}$$

where:

C_{10} and K are coefficients of the Neo-Hookean material model.

2.1.3. Arruda-Boyce model

This material model is available for 2D, brick and tetrahedral elements. The Arruda-Boyce material model is a hyperelastic material model used to model rubber materials. The implementation of this model follows the Ogden material behavior for volume-preserving deformation modes. Based

Preprints (www.preprints.org) | NOT PEER-REVIEWED | Posted: 13 January 2021 doi:10.20944/preprints202101.0241.v1

on the molecular chain network, it is also called the Arruda-Boyce 8-chain model because it was developed based on a representative volume (hexahedron) element, where 8 chains emanate from the centre to the corners of the volume. This is a two- parameter shear model based only on I_1 and works well with limited test data. The potential function of the material is as follows:

$$W = \mu \sum_{i=1}^{5} \frac{C_i}{\lambda_m^{2i-2}} \left(\overline{I_1^i} - 3^i \right) + K \left(\frac{J_3{}^2 - 1}{2} - \ln J_3 \right) \tag{14}$$

2.1.4. Ogden model

Proposed in 1972 by Ogden, this is also a phenomenological model and is based on principal stretches instead of invariants. The model is able to capture upturn (stiffening) of the stress-strain curve and models rubber accurately for large ranges of deformation. This material model is available for 2D, brick, tetrahedral, membrane and shell elements. The Ogden material model is a hyperelastic material model that has three material constants. The software supports up to a sixth-order variant. The potential function of the Ogden material is as follows:

$$W = \sum_{i=1}^{N} \frac{\mu_i}{\alpha_i} \left(\overline{\lambda_1^{\alpha_i}} + \overline{\lambda_2^{\alpha_i}} + \overline{\lambda_3^{\alpha_i}} - 3 \right) + \sum_{i=1}^{N} \frac{K_i}{2} (J_3 - 1)^{2i} \tag{15}$$

If N=2, α_1=2, and α_2=-2, the Mooney-Rivlin material model is obtained. If N=1 and α_1=2, Ogden's model degenerates to the Neo-Hookean material model. In the Ogden form the initial shear modulus, μ_0, depends on all the coefficients:

$$\mu_0 = \frac{1}{2} \sum_{i=1}^{N} \mu_i \alpha_i \tag{16}$$

2.2. Experimental details

The method applied in this study consisted in the analysis of selected equations of the hyperelastic material models in terms of the material data for the ball shelling obtained from uniaxial tensile tests. The data collection process followed the requirements of the PN-ISO 34-1:2007 standard, which specifies the testing conditions. Empirical tests on ball shelling samples were performed using an INSTRON-5840® strength testing machine equipped with software recording testing data, additionally using an extensometer **Figure 2**. In order to eliminate the potential effect of the direction of basketball shelling sampling on the recorded results the direction of sample circumferential collection was varied. Tests were conducted on 10 dumbbell specimens.

Preprints (www.preprints.org) | NOT PEER-REVIEWED | Posted: 13 January 2021 doi:10.20944/preprints202101.0241.v1

Figure 2. An uniaxial tensile specimen mounted on the testing machine.

Specimens were subjected to tension tests at 100 mm/min. The testing procedure was recorded using a video camera with the originally developed DIC system [**12-14**]. The recorded parameters included the increment in tensile force F[N], the increment in length *l*=[mm] and strain *ε* [-]. Geometrical dimensions of the tested specimens are presented in **Figure 3**.

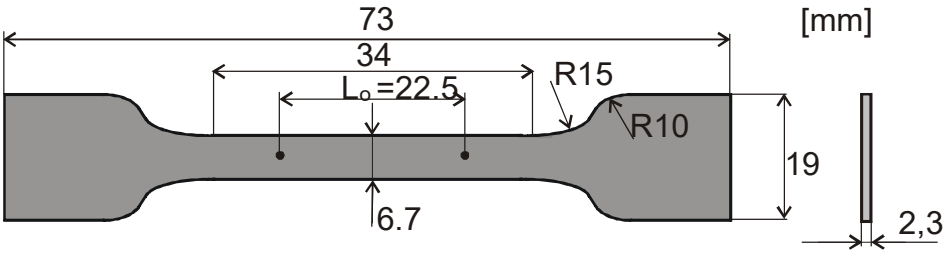

Figure 3. Dimensions of specimens

Optical methods to measure strains are best suited for such applications, since measurement is taken remotely, without interfering with the flexible geometry of specimens or any additional loading. Many researchers [**15-19**] have applied a similar technique to measure strains in hyperelastic rubber-like materials. Experimental results and analytical calculations were averaged and they are presented in the graph in **Figure 4**. Force was recorded in the function of specimen elongation until specimen failure. Points in the graph are experimental values, while the approximation line identifies the fitting function given in the equation form. Results cover the range of loads from the zero value of initial loading up to the tensile strength limits for ball shelling reinforced fibres. The averaged value of failure load was F=72.5 N, which corresponded to elongation strain ε = 7.7%. In practice this reflects the ultimate rupture strength of ball shelling under the influence of internal pressure.

Preprints (www.preprints.org) | NOT PEER-REVIEWED | Posted: 13 January 2021 doi:10.20944/preprints202101.0241.v1

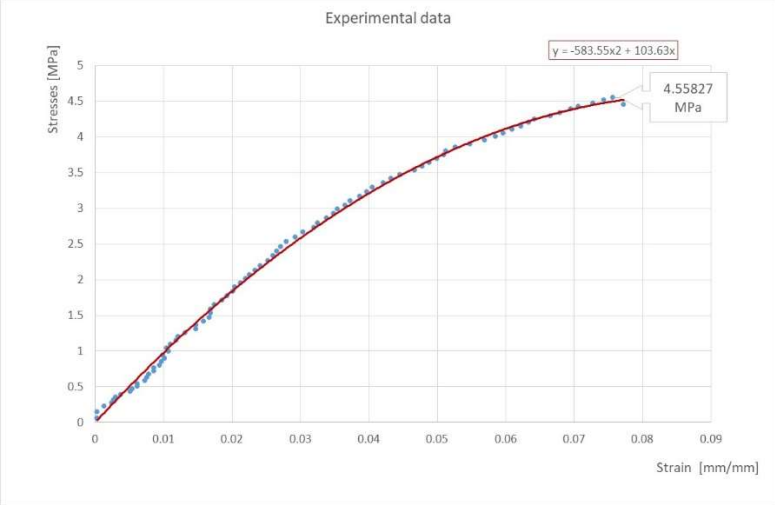

Figure 4. The curve of averaged stress-strain characteristics of the basketball shelling rubber-based material.

Having the strain-stress strength characteristics of the ball shelling to determine calculation factors of the equation the so-called curve fitting method was applied by trial and error. This approach is based on the intuitive introduction of coefficient values of a given phenomenological model. Another solution is to use an appropriate computational tool such as e.g. an open-source Hyperfit® programme [**20**] **Figure 5**.

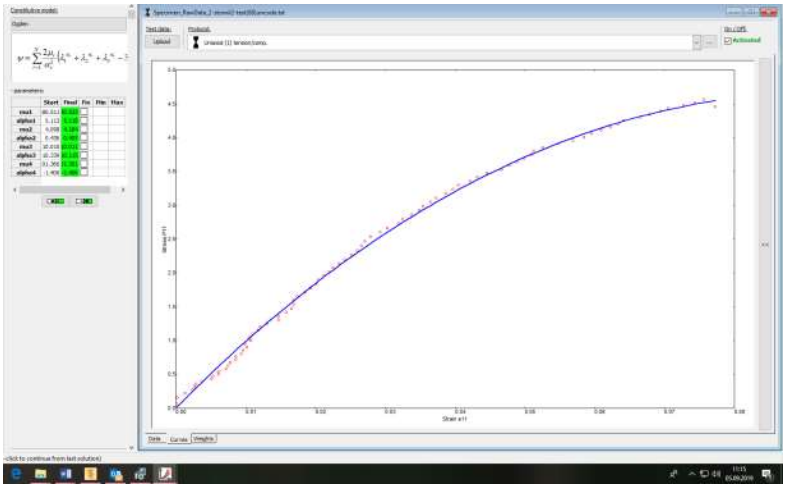

Figure 5. The Selection window of the Hyperfit® computer programme.

After the introduction of experimental data and the selection of an appropriate model for hyperelastic materials the programme automatically fits the regression curve and determines the computational coefficients of the polynomial. The programme also makes it possible to compare several different hyperelastic models, thus facilitating the selection of an optimal model for a given set of experimental data.

In the case of modelling in the FEM numerical environment the experimental data may be directly implemented to the computer programme, in which simulation analyses are conducted [**21**]. For this purpose, the first step was to use a specific programme facilitating the construction of virtual geometry for the ball shelling specimen. The Inventor Professional ver. 2017® was used and a 3-D

Preprints (www.preprints.org) | NOT PEER-REVIEWED | Posted: 13 January 2021 doi:10.20944/preprints202101.0241.v1

geometrical model was constructed. This model was supplemented with data on the material and further strength analysis could be conducted in the simplified version of this programme. It was decided to perform analyses in a more advanced environment and the Autodesk Simulation Mechanical® programme was used **Figure 6**.

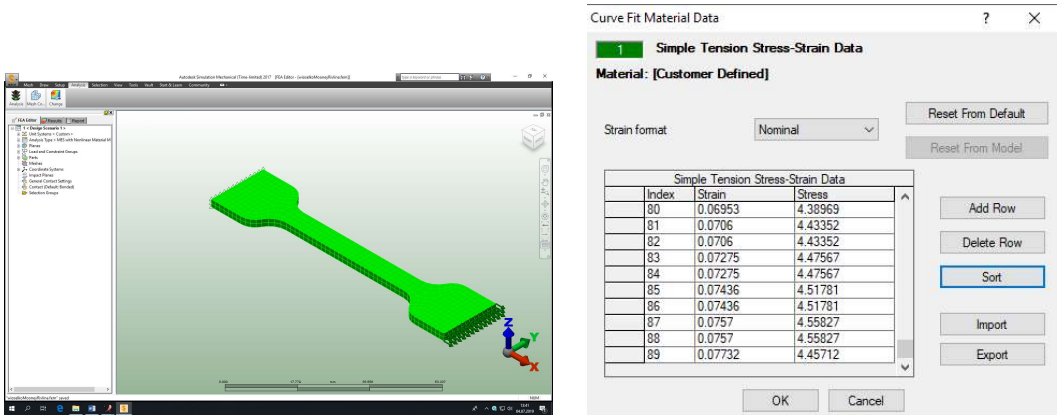

Figure 6. The Selection Window of the Autodesk Simulation Mechanical 2017® programme.

Depending on the used material models in the finite element method (FEM) curves more or less convergent with experimental data are obtained. In reality in no case the model curve in a given hyperelastic material model overlapped ideally with the experimental curve. In practice it is attempted to minimise them and to select an optimal material model. The best method to verify the selection of an accurate material model is to conduct a comparative analysis of results provided by the FEM numerical simulation with experimental data at an identical loading level. It is generally assumed that the results obtained from simulation are correct if the error does not exceed 5% in relation to the data from the conducted experiment.

2.2.1. Experimental results and curve fitting for FEM self selection

In the first stage of numerical calculations the task was to select appropriate hyperelastic material models offered in the FEM calculations. Four material models were selected from the Autodesk Simulation Mechanical ver. 2017® programme. The best method verifying the selection of an accurate material model is to perform a comparative analysis of results from FEM numerical simulation and experimental data, assuming the same loading level. Virtual models were loaded similarly as specimens in experimental tests with the tensile force F = 72.5 N, being a mean value of actual load. The virtual numerical model of the dumbbell specimen consisted of 900 Brick type finite elements comprising 4869 nodes. Results of the numerical calculations in selected material models are presented in the form of displacements in **Figure 7**, and the degree of goodness of fit for the regression curve with material constants in **Figure 8**.

Preprints (www.preprints.org) | NOT PEER-REVIEWED | Posted: 13 January 2021 doi:10.20944/preprints202101.0241.v1

a)

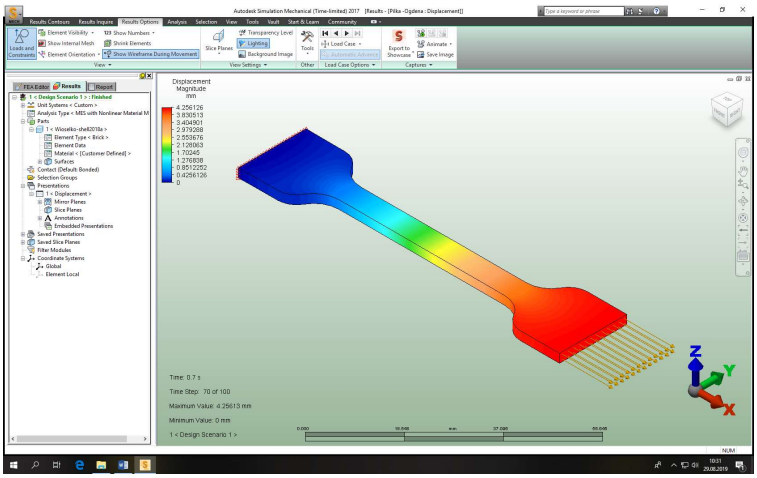

b)

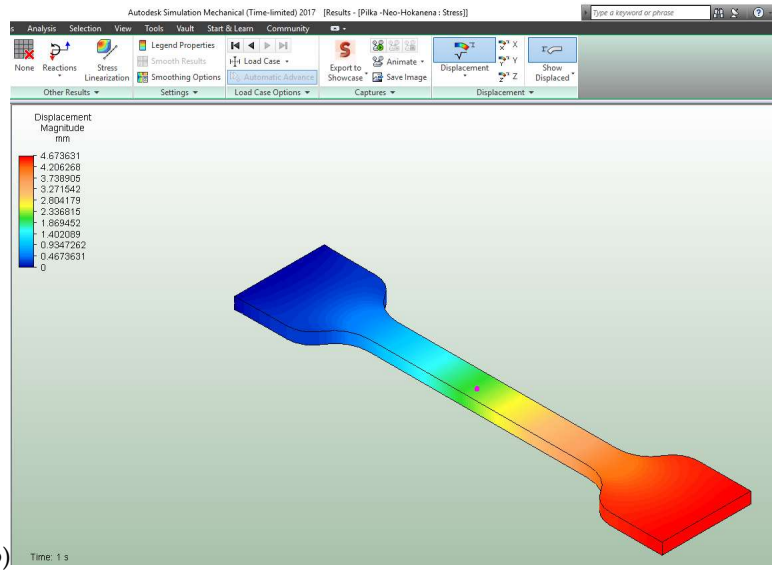

c)

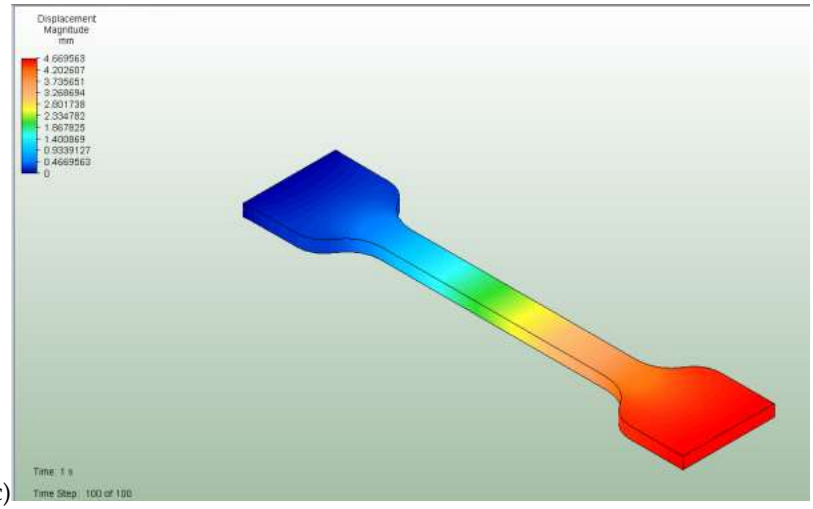

Preprints (www.preprints.org) | NOT PEER-REVIEWED | Posted: 13 January 2021 doi:10.20944/preprints202101.0241.v1

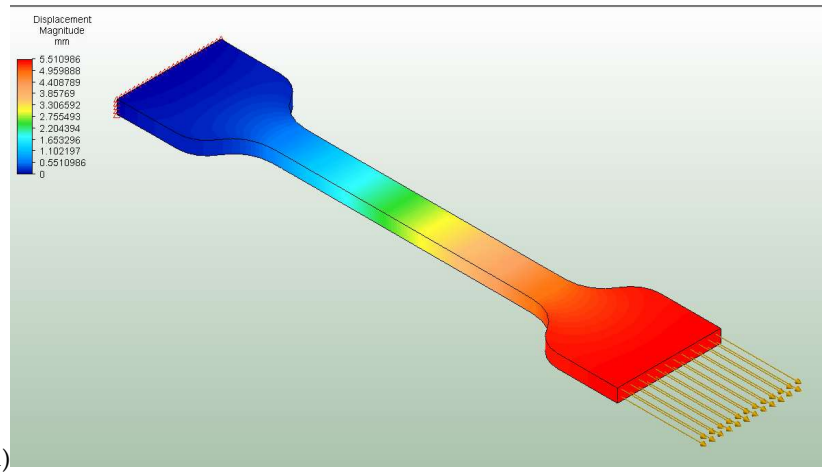

d)

Figure 7. Calculated displacements in the computer simulation for: **a)** Ogden, **b)** neo-Hookean, **c)** Arruda-Boyce, **d)** Mooney-Rivlin models.

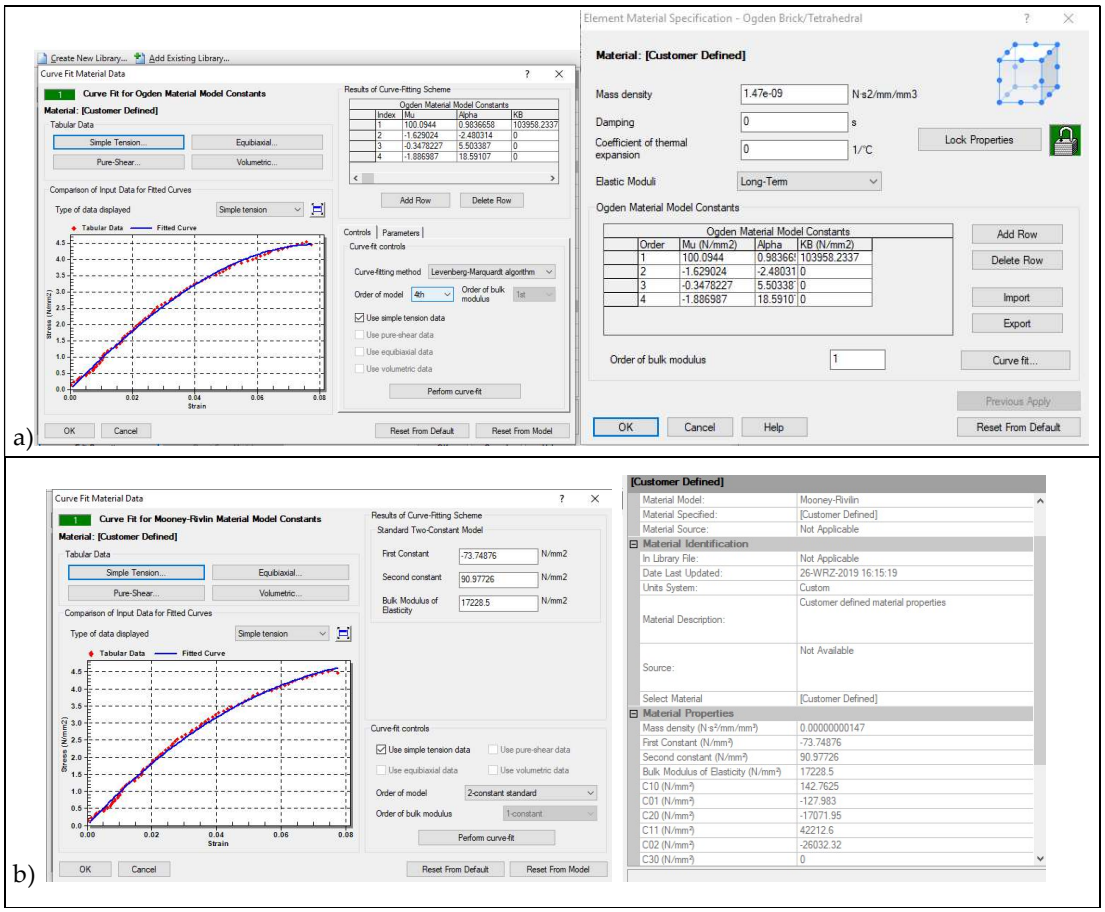

Preprints (www.preprints.org) | NOT PEER-REVIEWED | Posted: 13 January 2021 doi:10.20944/preprints202101.0241.v1

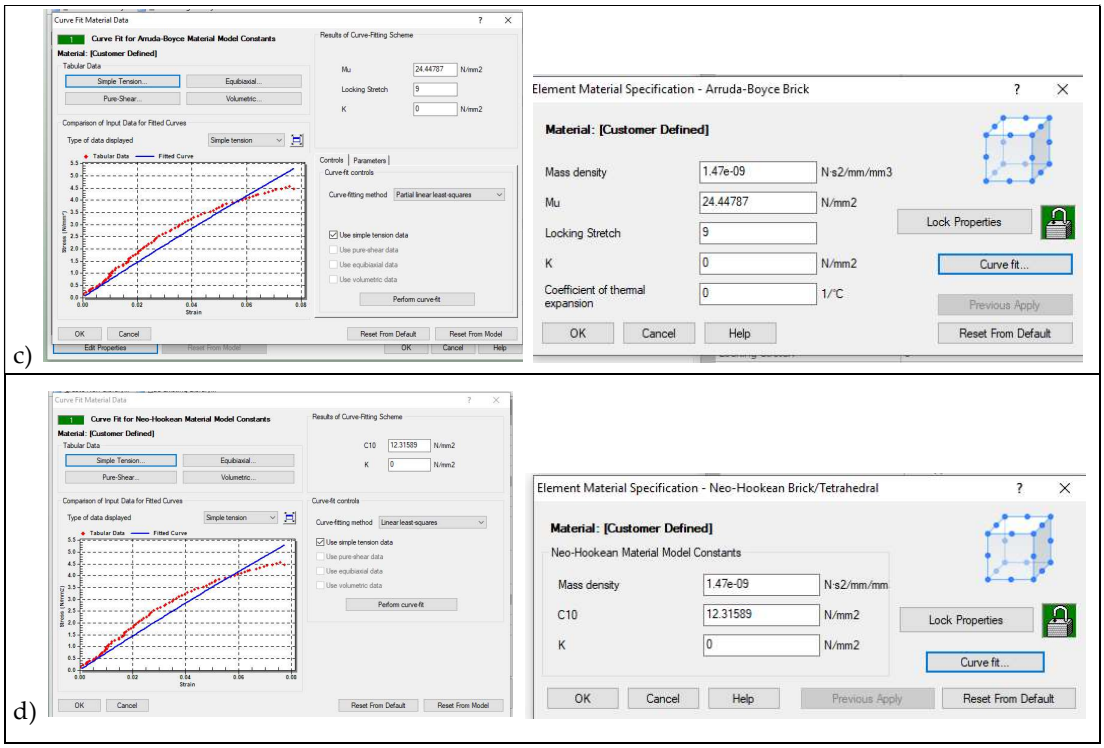

Figure 8. Selection windows for regression curves and calculated values of material constants for selected simulation models: **a)** the Ogden model, **b)** the Mooney-Rivlin model, **c)** the Arruda-Boyce model, **d)** neo-Hookean model.

Table 1. Experimental and simulation data from the Autodesk Simulation Mechanical 2017® (Load F= 72,5N)

	Type of analysis							
	Experimental	FEM models						
Parameter		neo-Hookean	Mooney-Rivlin		**Ogden model**		Arruda-Boyce	
$\Delta l[mm]$	4.404	4.673 (5.7%)	5.511	(20%)	**4.256**	**(3.36%)**	4.669	(5.7%)
ε	0,077	0.085 (9.4%)	0.030	(61%)	**0.079**	**(2.59%)**	0.083	(7.2%)
σ[MPa]	4.728	6.503 (27%)	4.923	(4.0%)	**4.862**	**(2.8%)**	6.996	(3.2%)

Experimental and numerical results are given in **Table 1**. Based on the analysis of these results an appropriate hyperelastic material model was selected for the ball shelling. The Ogden material model was selected as that showing goodness of fit for the regression curve **Figure 8a**. At the same time this model has the lowest deviation values of the comparison error (presented as percentages in parentheses) in **Table 1**. This model seems to be the correct choice among the available material models in view of its ability to match fit the experimental stress-strain results at low strain levels. Results of the other numerical calculations in the stress-strain function in the form of bitmaps for the selected Ogden model are shown in **Figure 9**.

Preprints (www.preprints.org) | NOT PEER-REVIEWED | Posted: 13 January 2021 doi:10.20944/preprints202101.0241.v1

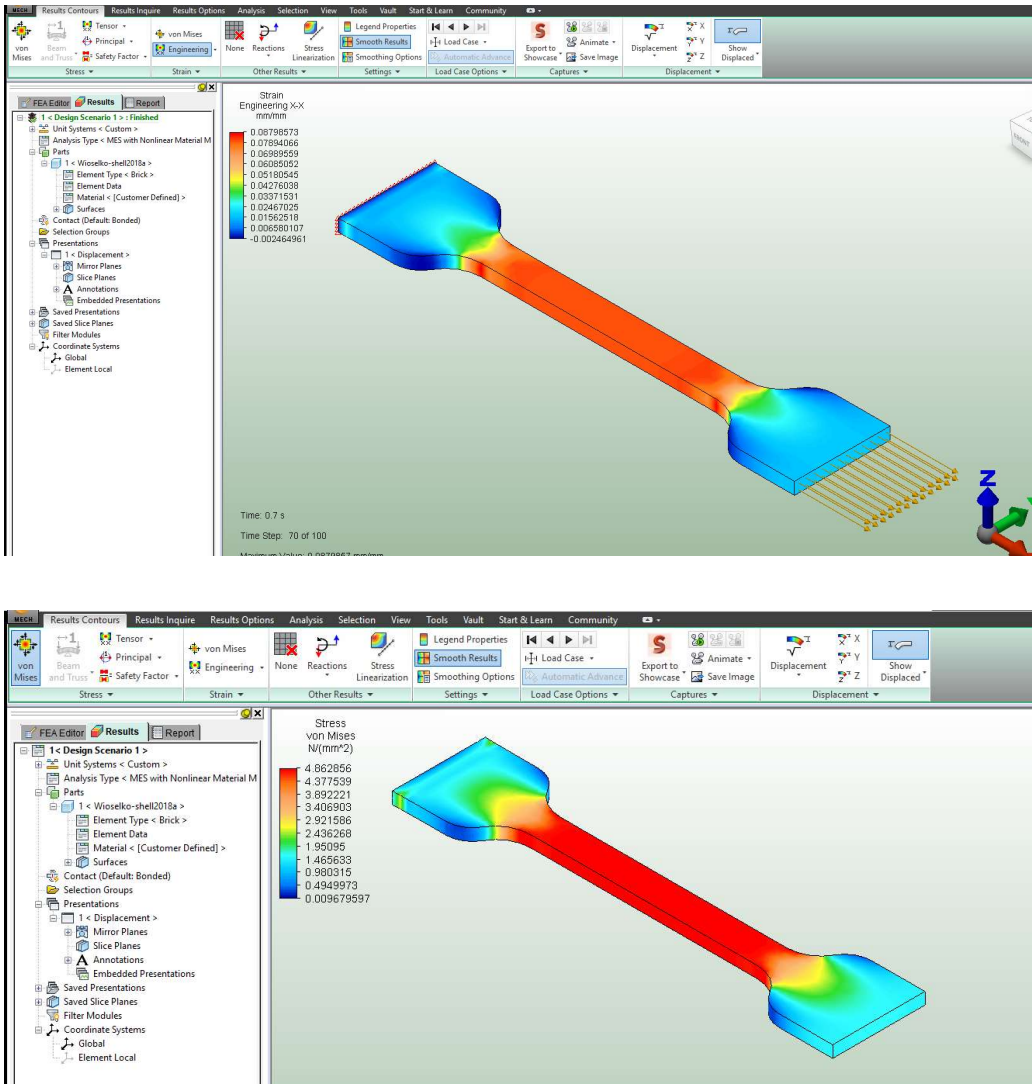

Figure 9. The image of unit strains and reduced stresses in the Ogden material model.

2.3. *A Basketball and its Modelling Using the Finite Element Method (FEM)*

Most indoor sports disciplines are practiced on the floor using a ball (shown in **Figure 10**). For this reason, an important parameter defining suitability of a given floor for these sports is provided by the value of ball rebound.

Preprints (www.preprints.org) | NOT PEER-REVIEWED | Posted: 13 January 2021 doi:10.20944/preprints202101.0241.v1

Basketball parameters
(mean values)
Size 7
diameter - D = 240 [mm]
circumference - L = 754 [mm]
mass - 0,597 [kg]
density - 1.47 [g/cm^3]
shell thickness - 2.4 [mm]
mass damping coefficient - 0,1

Figure 10. A photo of a standard basketball Kipsta ® and its parameters

Equipment used to test the vertical behaviour of the ball was designed according to the PN-EN 12235 standard requirements. When determining this value in practice a gauging apparatus measures the velocity of an acoustic wave propagation in the air are shown in **Figure 11**. The measurement is based on the time passing between successive acoustic impulses, i.e. between the first and second impact during ball rebound from the floor. The equipment releasing the ball was mounted at an initial height from the floor H ($1.80 \pm 0.01\ m$).

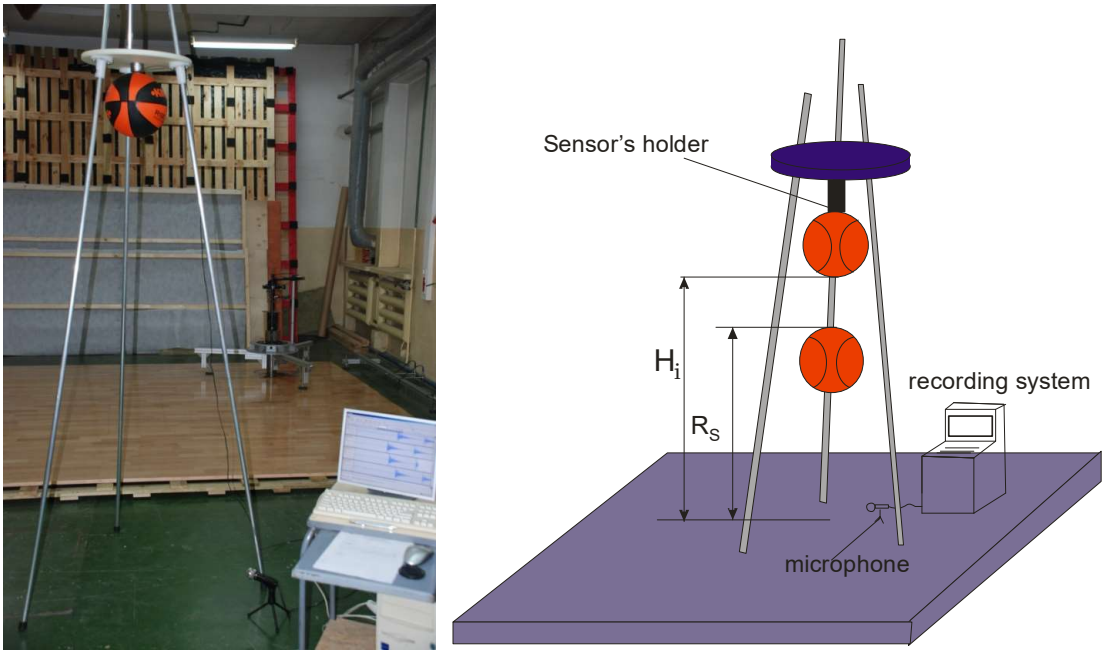

Figure 11. Equipment used for testing the vertical behaviour of the basketball

The testing stand is composed of a device to which a ball is attached, a microphone and a measuring apparatus recording the course of the process. The vertical fall of a ball from a specific height in the potential field is described by uniformly accelerated motion. When neglecting the effect of air resistance this motion may be described by a formula:

$$H_i = \frac{gt^2}{2} \tag{17}$$

Preprints (www.preprints.org) | NOT PEER-REVIEWED | Posted: 13 January 2021 doi:10.20944/preprints202101.0241.v1

where: t - time [s], g = 9.81 m/s^2

Substituting t = 0.5T we obtain:

$$R_s = 1.23 \cdot T^2 \tag{18}$$

Applying the phenomenon of propagation of the acoustic wave in the air and after modification based on the PN-EN 12235 standard to formula **(**17**)** we may determine the height of vertical rebound of a ball from the floor:

$$R_s = 1.23 \cdot (T - K)^2 [\mathrm{m}] \tag{19}$$

where: K – correction factor in accordance with the above-mentioned standard is 0.025s for UEFA or without K for EN 12235.

Knowing the time measured by the apparatus we may estimate averaged values of ball rebound from the floor. Empirical tests were conducted under constant climatic conditions and at a constant temperature of internal pressure of gas (the air) in the ball p = 0.06 MPa. The actual basketball should meet the requirements specified by FIBA. According to the official FIBA basketball rules [**22**], basketballs have to be inflated to an air pressure such that, when they are dropped onto the playing floor from a height of approximately 1800 mm measured from the bottom of the ball, they will rebound to a height of between 1200 and 1400 mm, measured to the top of the ball. The vertical ball behavior for these types of floor has to fulfill the requirements of EN 12235. According to this technical requirement, a standard basketball, which drops from a height of 1800 mm, has to have a relative rebound height of at least 90% of the rebound height on concrete. The basketball rebound height(R) on the tested floors is calculated in % by Equation:

$$R = \frac{R_S}{R_C} \cdot 100\% \tag{20}$$

Where: R_s is the rebound height from the sports surface, in metres,

R_c is the rebound height from concrete, in metres.

The reference value height (R_c) corresponding to the bounce height measured on concrete floor was 1.2 m R% - the value has to be at least 90% of the reference value height according to EN 12235, corresponds to the target height of 1.083 m. In the case of collision of a ball with a rigid surface of the floor, the ball will deform during the impact. Ball deformation affects the height of the rebound. It is dependent e.g. on such factors as the type of ball and flooring materials and internal pressure of the ball, while it is indirectly influenced by the free fall height, temperature, etc. These dependencies have a significant effect on dissipation of energy, defined by the coefficient of restitution (COR) [**23-26**] expressed by the equation:

$$e = \frac{v_2}{v_1} = \sqrt{\frac{R_S}{H}} \tag{21}$$

where : $v_1$and v_2 are the inbound and rebound speeds, respectively

In order to provide an accurate prediction of behaviour for the rubber sheathing of a basketball used in the testing system (e.g. bounce from a stiff floor) using the finite element simulation, the ball should be tested under the same loading conditions as those applied in the original basketball-floor system. The performed validation of the numerical hyperelastic models using experimental data made it possible to select an optimal model material for the construction of an appropriate virtual model of a basketball in the computer programme, as shown in **Figure 12**.

Preprints (www.preprints.org) | NOT PEER-REVIEWED | Posted: 13 January 2021 doi:10.20944/preprints202101.0241.v1

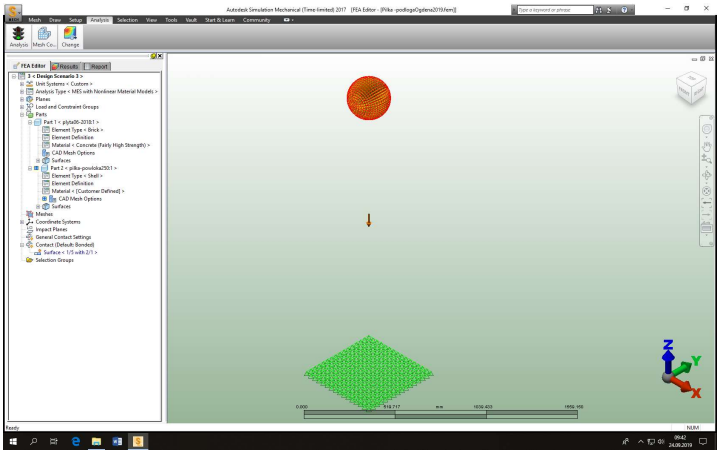

Figure 12. The FEM model of the ball and surface.

Simulation analyses were conducted in the Autodesk Simulation Mechanical® programme in the non-linear calculation environment. The model of the basketball shell material was modelled to exhibit hyperelastic properties corresponding to the Ogden model. Thus 8-node Shell-type finite elements were used to model the ball shell. The rigid floor was modelled as a material of Concrete High Strength from the library of the computational programme. The geometric model of the rigid floor was digitised using 8-node Brick-type finite elements. The FEM simulation was performed by assuming a free fall of the ball model with the internal pressure of 0.6 bar onto a floor from a similar height as that of the actual ball as shown in Figure 13. In simulation analyses the Rayleigh damping coefficient of 0.45 was assumed. Geometrical and material data of the concrete floor model are presented in **Table 2**.

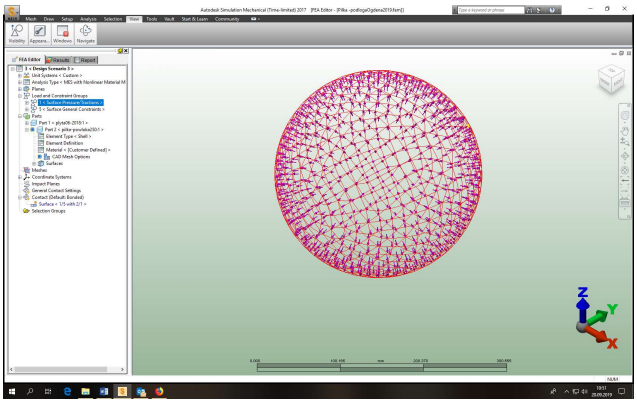

Figure 13. The image of applied internal pressure in the ball model

Table 2. Data concrete

Floor parameters (concrete)
width - 500 mm
length - 500 mm
thickness - 40 mm
density – 2.35[g/cm^3]
modulus of elasticity E =20684[MPa]
Poisson's ratio - $\nu = 0.15$
damping ratio - 0.3

3. Results and discussion

Numerical simulations for the rebound of a ball model from the rigid surface were performed for two selected materials. The free fall of the ball onto the surface was executed from different heights. The surface for the rebound was made from concrete and beech wood. Averaged rebound results from different free fall heights (Hi) under constant climatic conditions and constant internal pressure of gas (air) in the ball p = 0.06 MPa are presented in a graph in **Figure 14**. The rebound value was measured at the top of the ball.

Preprints (www.preprints.org) | NOT PEER-REVIEWED | Posted: 13 January 2021 doi:10.20944/preprints202101.0241.v1

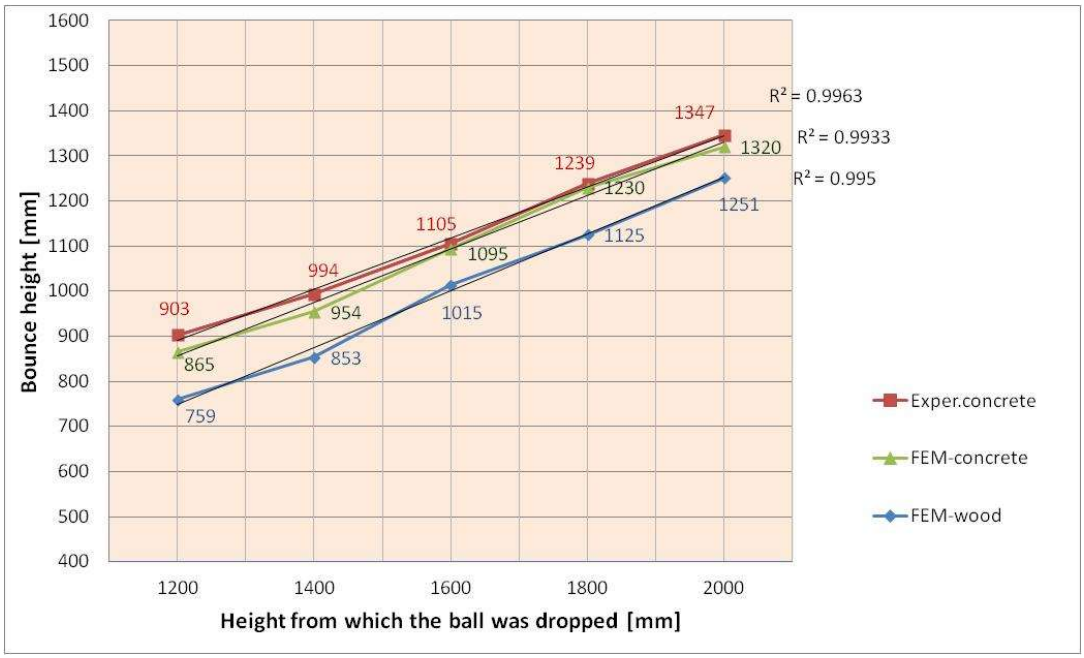

Figure 14. Results of numerical calculations and experimental data for ball rebound height

Based on the analyses of the study results the coefficient of restitution COR was calculated according to formula (21) as approx. 0.7. It is a rebound amounting to 70% height of the ball free fall or its model onto a hard rigid surface. The COR value defines dissipation of energy when the ball hits the floor. Energy is dissipated into heat energy, sound and the friction force resulting from the contact of the ball surface and the floor. Its value is dependent on the type of flooring material and decreases with an increase in the fall height. At the moment of contact of the ball with a rigid surface the ball is subjected to impact and the centre of inertia attempts to move while the floor surface attempts to stop it. This leads both to an elastic deformation of the ball and the floor surface, as well as the generation of slight friction forces inside the ball. Thus a small portion of the energy is dissipated as friction energy. The amount of friction energy depends both on compression of air inside the ball and the size of the contact surface between the ball and the floor. Although there is no lateral travel of the ball on the floor, theoretically small friction forces are generated as a result of the ball deformation and its contact with the floor surface. As a result of deformation the contact itself shifts from the point contact to surface contact depending on the character of the material. The contact surface of the ball with the floor is smaller in the case of rigid materials compared to viscoelastic materials. The graph of rebound is a linear function and data from numerical calculations are consistent with the experimental results. This indicates accuracy of the modelling process and adoption of an appropriate ball model in the computer programme. Simulation results for the rebound of the ball model are presented in **Figure 15**, while the rebound graph is given in **Figure 16**.

Preprints (www.preprints.org) | NOT PEER-REVIEWED | Posted: 13 January 2021 doi:10.20944/preprints202101.0241.v1

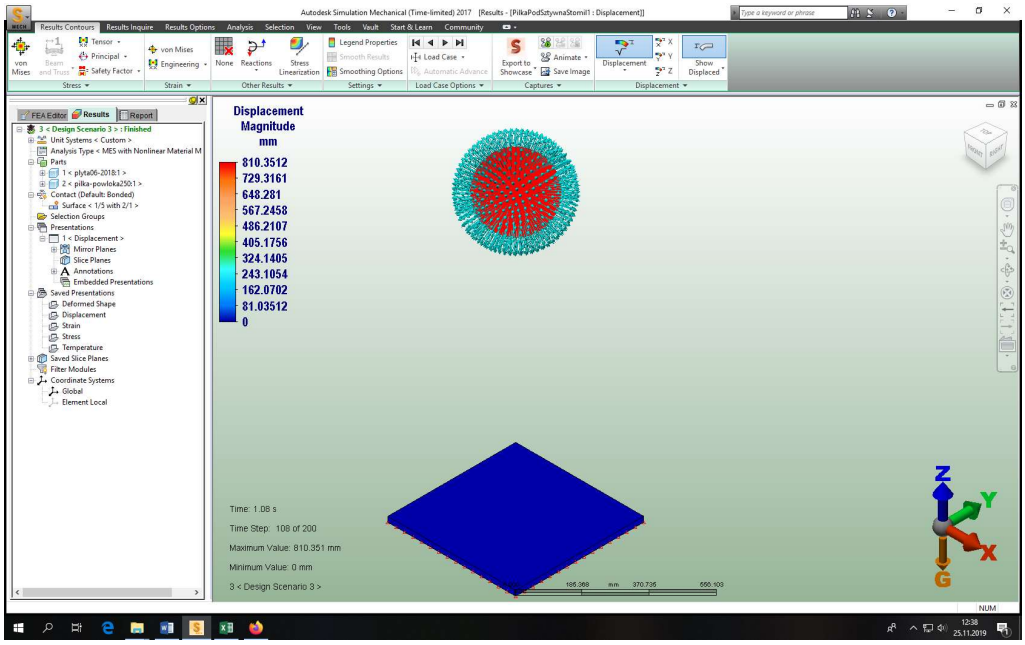

Figure 15. The image of numerical simulation of the first rebound of the ball model

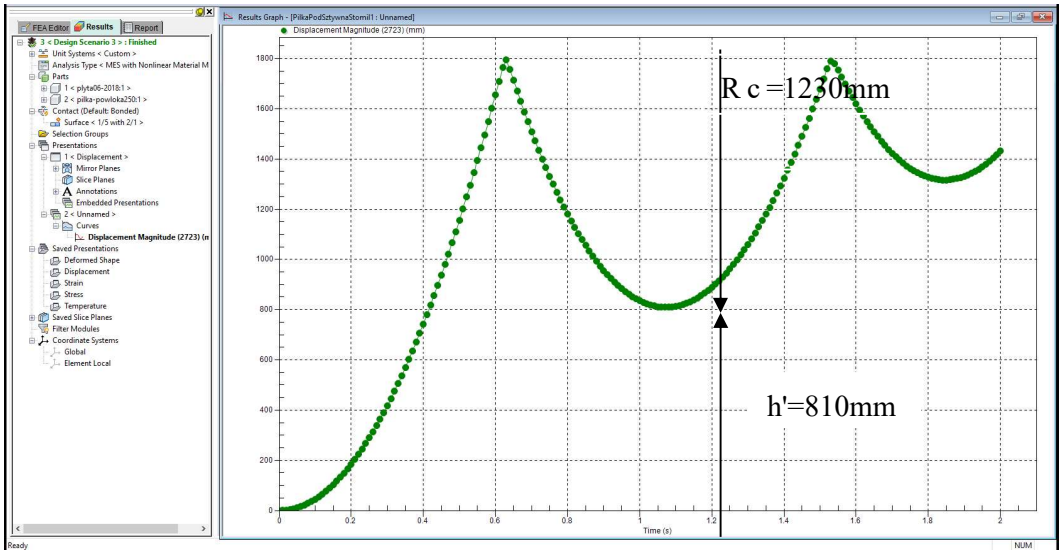

Figure 16. A graph of the ball model rebound calculations

The maximum value of the first rebound at the free fall of the ball model from a height of 1800 mm onto a model of a rigid floor (concrete) was R_c= 1230 mm. It is the total displacement of the ball model in the non-linear analysis from the initial position to time point of 1.08 s, when the model reaches the maximum height in the first rebound. The height of the first rebound is calculated according to the formula:

R_c = H-h'+D =1800 mm - (810+240) mm = 1230 mm

where: H – height of fall measured from the bottom of the ball model,

h' – height of rebound measured from the bottom of the ball model to a rigid floor,

D – diameter of the ball model = 240 mm

3. Conclusions

The mathematical description of behaviour of hyperelastic materials provides significant information concerning prediction of the response of the material at specific strain values, which characterise rubber-based materials. For this reason, the aim of this study was to determine non-linear hyperelastic mechanical properties of the basketball shell material as well as behaviour of the FEM ball model during simulation analyses in the process of ball rebound from a rigid floor. In order to specify these material data, it was necessary to conduct laboratory tests. The performed analysis of applicability of hyperelastic material models to describe the behaviour of a rubber-based basketball shell material under uniaxial tension gave positive results.

1. Based on data from these tests the Ogden material model was selected, which precisely matched the regression curve from the results obtained from experimental tests.
2. The positively verified material model was next used to model material properties of the ball shell model in the simulation FEM programme. The simulation programme included the defined ball shell material model as well as initial conditions in the form of internal pressure, values of free fall identical to that under actual conditions and neglected the effect of air resistance (drag).
3. As a result of FEM calculations the characteristics of ball model rebound were obtained and they were consistent with experimental data. The data from these calculations did not diverge from the values recommended by FIBA guidelines.
4. Compared ball rebound results and those obtained from the FE model simulation in the form of the coefficient of restitution COR were reflected in the experimental results. The COR value decreased with an increase in the free fall height, similarly as an increase in velocity. For a hard rigid concrete floor this coefficient was highest in comparison to that of the wood surface.
5. Thus the less hard a given floor is at the behaviour of constant kinematic values and ball pressure, the lower the COR value is also going to be. As a consequence, more energy will be dissipated upon impact.

Frequently the selection of an appropriate test determines accuracy of the obtained results. It needs to be stressed that the FEM method is an approximate method burdened with a certain error. Nevertheless, the results provided by this method give a very good approximation to reality, while fine-tuning the model may reduce the number of extensive experimental tests. The obtained results of numerical modelling applying the finite element method may be used in future simulation studies on the behaviour of structural elements of sports floors.

Author Contributions: All authors have read and agreed to the published version of the manuscript

Conflict of interest: The authors declare no conflict of interest.

References

1. Mooney, M.A. A theory of large elastic deformation. *Journal of Applied Physics* **1940**, *11*, 582-592. http://dx.doi. org/10.1063/1.1712836.
2. Clanton, R.E.; Dwight, M.P. Team handball: step to success. *Hum Kinet* **1996**, 168-175.

3. Mooney, M.A. A theory of large elastic deformation. *Journal of Applied Physics* **1940**, *11*(9),582-592. http://dx.doi.org/10.1063/1.1712836.

4. Ogden, R.W. et al. Fitting hyperelastic models to experimental data. *Computational Mechanics* **2004**, *34*, 484-502.

5. Yeoh, O.H. Some form of strain energy functions for rubber. *Rubber Chemistry and Technology* **1993**, *66*(5), 754-771. http:// dx.doi.org/10.5254/1.3538343.

6. Rivlin, R.S. Large elastic deformations of isotropic materials I. *Fundamental concepts. Philosophical Transitions of the Royal Society of London A* **1948**, *240*(822), 459-490.

7. Arruda, E.M and Boyce, M.C. A three-dimensional constitutive model for the large stretch behaviour of rubber elastic materials. *Journal of the Mechanics and Physics of Solids* **1993,** *41*(2), 389- 412. http://dx.doi.org/10.1016/0022-5096(93)90013-6.

8. Dolwichai, P.; Limtragool, I.; Inban, S.; Piyasin, S. Hyperelastic Material Models for Finite Element Analysis with Commercial Rubber. *Technology and Innovation for Sustainable Development Conference TISD.* Khon Kean University. Thailand. **2006**, 769-774.

9. Ogden, R.W. Elasticity and inelasticity of rubber. Mechanics and thermomechanics of rubberlike solids. *CISM Couses and Lect. Springer* **2014**, 452, 134-185.

10. Brinson, H and Brinson, L. Polymer engineering science and viscoelasticity: an introduction. *Springer* **2008**, Evanston.

11. Ali, A. Hosseini, M and Sahari, B.A. A review of constitutive models for rubber-like materials. *American Journal of Engineering and Applied Sciences* **2010**, 3(1),232-239. http:// dx.doi.org/10.3844/ajeassp.2010.232.239

12. Chevalier, L.; Calloch, S.; Hild, F. and Marco, Y. Digital image correlation used to analyze the multiaxial behavior of rubber-like materials. *European Journal of Mechanics. A, Solids*. **2001**, *20*(2),169-187. http://dx.doi.org/10.1016/S0997-7538(00)01135- 9.

13. Alireza, K.; Susumu, K.; Reza, R.; Mahdi, N. Measurement of the mechanical properties of the handball, volleyball, and basketball using DIC method: a combination of experimental, constitutive, and viscoelastic models. Sport Sciences for Health, **2015**, DOI 10.1007/s11332-015-0240-2, researchgate.net/publication/282182703

14. Sasso, M.; Palmieri, G.; Chiappini, G. and Amodio, D. Characterization of hyperelastic rubber-like materials by biaxial and uniaxial stretching tests based on optical methods. *Polymer Testing* **2008**, *27*(8), 995-1004. http://dx.doi.org/10.1016/j. polymertesting.2008.09.001.

15. Bradley, G.L; Chang, P.C and McKenna, G.B. Rubber modeling using uniaxial test data. *Journal of Applied Polymer Science* **2001,** *81*(4),837-848. http://dx.doi.org/10.1002/app.1503.

16. Beda, T. An approach for hyperelastic model-building and parameters estimation a review of constructive models. *European Polymer Journal* **2014**, 50(1), 97-108.

17. Martins, P.; Jorge, R.N.; Ferreira, A. A comparative study of several materials models for prediction of hyperelastic properties: application to silicone-rubber and soft tissues. *Strain* **2006**, *42*, 135-147.

18. Ogden, R.W. Large deformation isotropic elasticity— on the correlation of theory and experiment for the incompressible rubber-like solids. *Proceedings of the Royal Society of London. Series A, Mathematical and Physical Sciences* **1972**, *326*(1567), 565- 584. http://dx.doi.org/10.1098/rspa.1972.0026.

19. Palmieri, G.; Chiappini, G.; Sasso, M. and Papalini, S. Hyperelastic material characterization by planar tension tests and full-field strain measurement. In: *Proceedings of the SEM Annual Conference,;* Albuquerque, Mexico. Albuquerque: Society for Experimental Mechanics, **2009**.

20. Daniel de Bartoli at al. HYPERFIT - Curve fitting software for incompressible hyperelastic material models. *21st Brazilian Congress of Mechanical Engineering* **2011**, Natal, RN, Brazil.

21. Marczak, R.; Hoss, L.; Gheller, Jr. J. Elastomer Characterization for Numerical Analysis. SENAI-RS, Porto Alegre, Portugal **2006**, 126.

22. FIBA Central Board. Official basketball rules. *Basketball equipment. Mies, Switzerland* **2017.** http://www.baske tball.ca Accessed 8 May 2018

23. Cross, R. The bounce of a ball *American Journal of Physics* **1999**, *67*, 222-227.

24. Aryaei A.; Hashemnia K and Jafarpur K. Experimental and numerical study of ball size effect on restitution coefficient in low velocity impacts *International Journal of Impact Engineering.* **2010**, *37* 1037-1044.

25. Cross, R. Measurements of the horizontal and vertical speeds of tennis court. *Sports Engineering* **2003,** *6*, 95-111.

 doi:10.20944/preprints202101.0241.v1

26. Njock-Libiii, J. Applying dynamics to the bouncing of game balls: experimental investigation of the relationship between the duration of a linear impulse during an impact and the energy dissipated. *American Society for Engineering Education* **2012**, AC 2012-2947.

27. PN-EN-12235:2013. *Surfaces for sports areas* – determination of vertical ball behaviour.